Sébastien Briot
Vigen Arakelian
Département de Génie Mécanique et Automatique –
L.G.C.G.M. EA3913,
Institut National des Sciences Appliquées (I.N.S.A.),
20 avenue des Buttes de Coësmes – CS 14315,
F-35043 Rennes, France
sebastien.briot@ens.insa-rennes.fr
vigen.arakelyan@insa-rennes.fr

Optimal Force Generation in Parallel Manipulators for Passing through the Singular Positions

Abstract

It is known that a parallel manipulator at a singular configuration can gain one or more degrees of freedom and become uncontrollable, that is, it might not reproduce a stable motion along a prescribed trajectory. However, it is proved experimentally that there is possible passing through the singular zones. This was simulated and shown through numerical examples and illustrated on several parallel structures. In this paper, we determine the optimal dynamic conditions generating a stable motion inside the singular zones. The obtained results show that the general condition for passing through a singularity can be defined as follows: the end-effector of the parallel manipulator can pass through the singular positions without perturbation of motion if the wrench applied on the end-effector by the legs and external efforts of the manipulator are orthogonal to the twist along the direction of the uncontrollable motion. This condition is obtained from the inverse dynamics and analytically demonstrated by the study of the Lagrangian of a general parallel manipulator. Numerical simulations are carried out using the software ADAMS and validated through experimental tests.

KEY WORDS—parallel manipulators, singularity, dynamics, force management, trajectory planning.

1. Introduction

Parallel manipulators have experienced an increase in popularity in recent years due to their higher rate of acceleration, payload-to-weight ratio, stiffness and low effective inertia compared with serial manipulators. However, they have some drawbacks, such as a small workspace and special singular zones within it. Thus, in the presence of singular positions, the workspace of the parallel manipulators, which is smaller than that of serial manipulators, becomes even smaller and limits their functional performance. The studies of singularity have reached different stages of development. The previous work on this problem is reported in a great number of publications and can be classified by different criteria. They can be arranged, for example, into three major groups, which are distinguished by historical evolution and are characterized by the method of study of the singularity, from kinematic, kinetostatic and dynamic points of view.

The physical interpretation of a singularity in kinematics refers to those configurations of parallel manipulators in which the number of degrees of freedom (DOF) of the mechanical structure changes instantaneously, either the manipulator gains some additional, uncontrollable DOF or loses some DOF. In this case the singularity analysis can be carried out on the basis of the properties of the Jacobian matrices of the mechanical structure (i.e. when the Jacobian matrices relating the input speeds and the output speeds become rank deficient (Gosselin and Angeles 1990; Ma and Angeles 1992; Ottaviano et al. 2001; Wen and Oapos Brien 2003)), by using Grassmann geometry (Merlet 1989) or screw theory (Hunt 1987; Bonev et al. 2003). However, it was observed that close to a singular configuration, a parallel manipulator loses its stiffness and its quality of motion transmission and, as a result, its payload capability. For this purpose, a kinetostatic approach has been applied for the evaluation of the quality of motion transmission in the singular zones of parallel manipulators. The quality of motion transmission of parallel manipulators was successfully studied by Kim and Choi (2001), Kim and Ryu (2004), Lee et al. (2002) and Weiwei and Shuang (2006). The quality of motion of manipulators with three DOF has been evaluated by means of a kinetostatic indicator, which is similar to the pressure angle (Alba-Gomez et al. 2005). Arakelian et al. (2008) used the pressure angle as an indicator of the quality of motion

The International Journal of Robotics Research
Vol. 27, No. 8, August 2008, pp. 967–983
DOI: 10.1177/0278364908094403

transmission and the nature of the inaccessibility of singular zones by parallel manipulators was shown.

The further study of singularity in parallel manipulators has revealed an interesting problem that concerns the path planning of parallel manipulators in the presence of singular positions, that is, the motion feasibility in the neighborhood of singularities. In this case the dynamic conditions can be considered in the design process. One of the most evident solutions for the stable motion generation in the neighborhood of singularities is to use redundant sensors and actuators (Collins and Long 1975; Dasgupta and Mruthyunjaya 1998a; Alvan and Slousch 2003; Glazunov et al. 2004). However, it is an expensive solution to the problem because of the additional actuators and the complicated control of the manipulator caused by actuation redundancy. Another approach concerns the use of motion planning to pass through the singularity (Nenchev et al. 1997; Bhattacharya et al. 1998; Dasgupta and Mruthyunjaya 1998b; Perng and Hsiao 1999; Hesselbach et al. 2004; Kemal Ider 2005; Kevin Jui and Sun 2005), that is, a parallel manipulator may track a path through singular poses if its velocity and acceleration are properly constrained. This is a promising method for the solution of this problem. Only a few research papers on this approach have addressed the use of path planning to obtain a good tracking performance, but they have not adequately addressed the physical interpretation of dynamic aspects.

In this paper the dynamic condition for passing through the singular positions is defined in general. It allows the stable motion generation inside in the presence of a singularity by means of the optimum force control. The disclosed condition can be formulated as follows. In the presence of a type 2 singularity, the platform of the parallel manipulator can pass through the singular positions without perturbation of motion if the wrench applied on the platform by the legs and external forces is orthogonal to the direction of uncontrollable motion. In other terms, the condition is that the work of applied forces and moments on the platform along the uncontrollable motion is equal to zero. This condition is obtained from the inverse dynamics and analytically demonstrated by the study of the Lagrangian of a general parallel manipulator. The obtained results are illustrated by numerical simulations and validated using experimental tests.

The paper is organized as follows. The next section presents theoretical aspects of the examined problem. Based on the Lagrangian formulation, the condition of force distribution is defined, which allows any of the parallel manipulators to pass through the type 2 singular positions. In Section 3, two applications illustrate the obtained theoretical results. In Section 4, the numerical simulations carried out using the software ADAMS are validated through experimental tests.

2. Optimal Dynamic Conditions for Passing through a Type 2 Singularity

Let us consider a parallel manipulator of m links, n DOF and driven by n actuators.

The Lagrangian dynamic formulation for a parallel manipulator can be expressed as

$$\boldsymbol{\tau} = \frac{\mathrm{d}}{\mathrm{dt}}\left(\frac{\partial L}{\partial \dot{\mathbf{q}}}\right) - \frac{\partial L}{\partial \mathbf{q}} + \mathbf{B}^{\mathrm{T}}\boldsymbol{\lambda}, \tag{1}$$

where: $\boldsymbol{\tau}$ is the vector of the input efforts; L is the Lagrangian of the manipulator; $\mathbf{q} = [q_1, q_2, ..., q_n]^{\mathrm{T}}$ and $\dot{\mathbf{q}} = [\dot{q}_1, \dot{q}_2, ..., \dot{q}_n]^{\mathrm{T}}$ represent the vector of active joints variables and the active joints velocities, respectively; $\mathbf{x} = [x, y, z, \phi, \psi, \theta]^{\mathrm{T}}$ and $\mathbf{v} = [\dot{x}, \dot{y}, \dot{z}, \dot{\phi}, \dot{\psi}, \dot{\theta}]^{\mathrm{T}}$ are trajectory parameters and their derivatives, respectively; x, y, z represent the position of the controlled point and ϕ, ψ and θ the rotation of the platform about three axes $\mathbf{a}_\phi$, $\mathbf{a}_\psi$ and $\mathbf{a}_\theta$; $\boldsymbol{\lambda}$ is the Lagrange multipliers vector, which is related to the wrench applied on the platform by

$$\boldsymbol{\lambda} = \mathbf{A}^{-\mathrm{T}}\mathbf{W}_\mathbf{p}, \tag{2}$$

where $\mathbf{A}$ and $\mathbf{B}$ are two matrices relating the vectors $\mathbf{v}$ and $\dot{\mathbf{q}}$ according to $\mathbf{A}\mathbf{v} = \mathbf{B}\dot{\mathbf{q}}$ (they can be found by derivating the closure equations with respect to time); $\mathbf{W}_\mathbf{p}$ is the wrench applied on the platform by the legs and external forces (Khalil and Guégan 2002), which is defined as

$$\mathbf{W}_\mathbf{p} = \left(\frac{\mathrm{d}}{\mathrm{dt}}\left(\frac{\partial L}{\partial \mathbf{v}}\right) - \frac{\partial L}{\partial \mathbf{x}}\right) = \begin{bmatrix} \mathbf{f}_\mathbf{p} \\ \\ \mathbf{n}_\mathbf{p} \end{bmatrix}, \tag{3}$$

where $\mathbf{f}_\mathbf{p}$ is the force along the directions of the global frame and $\mathbf{n}_\mathbf{p}$ is the torque about the axes $\mathbf{a}_\phi$, $\mathbf{a}_\psi$ and $\mathbf{a}_\theta$.

The term $\mathbf{W}_\mathbf{p}$ can be rewritten in the base frame using a transformation matrix $\mathbf{D}$ (Merlet 2006):

$$\mathbf{W}_\mathbf{p} = \mathbf{D}({}^{\mathbf{R}_0}\mathbf{W}_\mathbf{p}), \tag{4}$$

where ${}^{\mathbf{R}_0}\mathbf{W}_\mathbf{p}$ is the expression of the wrench $\mathbf{W}_\mathbf{p}$ in the base frame, and

$$\mathbf{D} = \begin{bmatrix} \mathbf{I}_{3\times 3} & \mathbf{0}_{3\times 3} \\ \\ \mathbf{0}_{3\times 3} & \mathbf{R}_{3\times 3} \end{bmatrix}, \tag{5}$$

where $\mathbf{I}_{3\times 3}$, $\mathbf{0}_{3\times 3}$ and $\mathbf{R}_{3\times 3}$ are, respectively, the identity matrix, the zero matrix and the transformation matrix between axes $\mathbf{a}_\phi$, $\mathbf{a}_\psi$ and $\mathbf{a}_\theta$ and the base frame, whose dimensions are 3×3.

By substituting (5) into (1), one can obtain

$$\boldsymbol{\tau} = \mathbf{W}_\mathbf{b} + \mathbf{J}^{\mathrm{T}\,\mathbf{R}_0}\mathbf{W}_\mathbf{p}, \quad \mathbf{W}_\mathbf{b} = \frac{\mathrm{d}}{\mathrm{dt}}\left(\frac{\partial L}{\partial \dot{\mathbf{q}}}\right) - \frac{\partial L}{\partial \mathbf{q}}, \tag{6}$$

where $\mathbf{J} = \left({}^{\mathbf{R}_0}\mathbf{A}\right)^{-1}\mathbf{B}$ is the Jacobian matrix between twist $\mathbf{t}$ of the platform (expressed in the base frame) and $\dot{\mathbf{q}}$, ${}^{\mathbf{R}_0}\mathbf{A} = \mathbf{AD}$ is the expression of matrix $\mathbf{A}$ in the base frame.

For any prescribed trajectory $\mathbf{x}(t)$, the values of vectors $\ddot{\mathbf{q}}$, $\dot{\mathbf{q}}$ and $\mathbf{q}$ can be found using the inverse kinematics. Thus, taking into account that the manipulator is not in a type 1 singularity (Gosselin and Angeles 1990), the terms $\mathbf{W_b}$ and ${}^{\mathbf{R}_0}\mathbf{W_p}$ can be computed. However, for a trajectory passing through a type 2 singularity, the determinant of matrix $\mathbf{J}$ tends to infinity. Numerically, the values of the efforts applied by the actuators become infinite. In practice, the manipulator is either locked in such a position of the end-effector or it generates an uncontrolled motion. That is, the end-effector of the manipulator could produce a motion, different to the prescribed trajectory.

It is known that a type 2 singularity appears when the determinant of matrix ${}^{\mathbf{R}_0}\mathbf{A}$ vanishes, in other words, when at least two of its columns are linearly dependant (Merlet 2006).

Let us rewrite the matrix ${}^{\mathbf{R}_0}\mathbf{A}$ as

$$ {}^{\mathbf{R}_0}\mathbf{A} = \begin{bmatrix} a_{11} & a_{12} & \dots & a_{16} \\ a_{21} & a_{22} & \dots & a_{26} \\ \vdots & \vdots & \ddots & \vdots \\ a_{61} & a_{62} & \dots & a_{66} \end{bmatrix}. \tag{7} $$

In the presence of a type 2 singularity the columns of the matrix ${}^{\mathbf{R}_0}\mathbf{A}$ are linearly dependant, that is,

$$ \sum_{j=1}^{6} \alpha_j a_{ij} = 0, \quad i = 1, \dots, 6, \tag{8} $$

where α_j are the coefficients, which in general can be functions of q_p ($p = 1, \dots, n$). It should be noted that the vector $\mathbf{t_s} = [\alpha_1, \alpha_2, \dots, \alpha_6]^{\mathrm{T}}$ represents the direction of the uncontrollable motion of the platform in a type 2 singularity.

Rewriting (8) in a vector form, we obtain

$$ \sum_{j=1}^{6} \alpha_j \mathbf{N}_j = \mathbf{0}, \quad \mathbf{N}_j = [a_{1j}, a_{2j}, \dots, a_{6j}]^{\mathrm{T}}, \quad j = 1, \dots, 6, \tag{9} $$

where $\mathbf{N}_j$ represents the jth column of the matrix ${}^{\mathbf{R}_0}\mathbf{A}$.

By substituting (9) into (2), we obtain

$$ \mathbf{N}_j^{\mathrm{T}}\boldsymbol{\lambda} = W_j, \quad j = 1, \dots, 6, \tag{10} $$

where W_j is the jth row of vector ${}^{\mathbf{R}_0}\mathbf{W_p}$.

Then, from (9) and (10) the following conditions are derived:

$$ \sum_{j=1}^{6} \left(\alpha_j \mathbf{N}_j^{\mathrm{T}}\boldsymbol{\lambda}\right) = \sum_{j=1}^{6} \left(\alpha_j W_j\right) = 0. \tag{11} $$

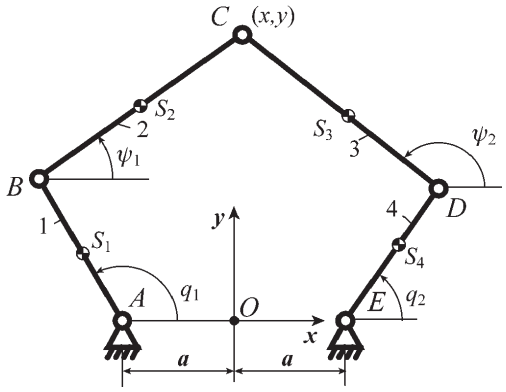

Fig. 1. Kinematic chain of the planar 5R parallel manipulator.

The term on the right-hand side of (11) corresponds to the scalar product of vectors $\mathbf{t_s}$ and ${}^{\mathbf{R}_0}\mathbf{W_p}$.

Thus, in the presence of a type 2 singularity, it is possible to satisfy conditions (11) if the wrench applied on the platform by the legs and external efforts ${}^{\mathbf{R}_0}\mathbf{W_p}$ are orthogonal to the direction of the uncontrollable motion $\mathbf{t_s}$. Otherwise, the dynamic model is not consistent. Obviously, in the presence of a type 2 singularity, the displacement of the end-effector of the manipulator has to be planned to satisfy (11).

Let us illustrate the considered problem by examples.

3. Illustrative examples

In this section, two examples are chosen to illustrate the obtained theoretical results discussed above. The first example presents a planar 5R parallel manipulator, which allows relatively simple mathematical models to be obtained to demonstrate the expected results using numerical simulations. The second example presents a parallel manipulator which was developed in the I.N.S.A. of Rennes. This example was chosen for validation of numerical simulations carried out by the software ADAMS on the built prototype.

3.1. Example 1: Planar 5R Parallel Manipulator

In the planar 5R parallel manipulator, as shown in Figure 1, the output point is connected to the base by two legs, each of which consists of three revolute joints and two links. In each of the two legs, the revolute joint connected to the base is actuated. Thus, such a manipulator is able to position its output point in a plane.

As shown in Figure 1, the actuated joints are denoted by A and E with input parameters q_1 and q_2. The common joint of the two legs is denoted by C, which is also the output point with controlled parameters x and y. A fixed global reference

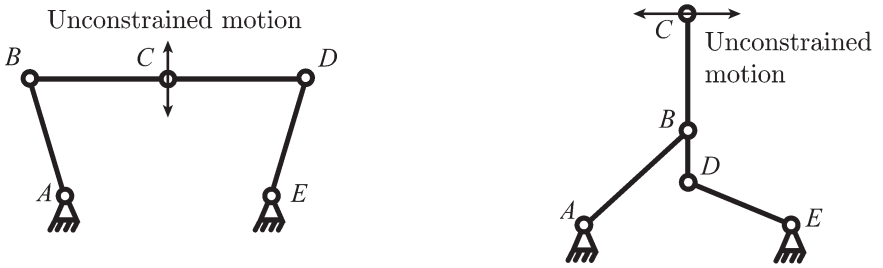

(a) $\psi_1 = \psi_2 \pm \pi$ (b) $\psi_1 = \psi_2$

Fig. 2. Second kind of singularities of the planar 5R parallel manipulator.

system ***xOy*** is located at the center of AE with the ***y***-axis normal to **AE** and the ***x***-axis directed along **AE**. The lengths of the links AB, BC, CD, DE are respectively denoted by L_1, L_2, L_3 and L_4. The positions of the centers of masses S_i of links from joint centers A, B, D and E are respectively denoted by dimensionless lengths r_1, r_2, r_3 and r_4, that is, $AS_1 = r_1 L_1$, $BS_2 = r_2 L_2$, $DS_3 = r_3 L_3$ and $ES_4 = r_4 L_4$.

The singularity analysis of this manipulator (Liu et al. 2006) shows that the type 2 singularities appear when legs 2 and 3 are in parallel (Figure 2).

In both cases, the gained degree of freedom is an infinitesimal translation perpendicular to legs 2 and 3. However, if $L_2 = L_3$, the gained degree of freedom in case (b) becomes a finite rotary motion about point B.

In order to simplify the analytic expressions, we consider that the gravity effects are along the z-axis and consequently the input torques are only due to inertia effects. To simplify the computation, it is also preferable to replace the masses of moving links by concentrated masses (Seyferth 1974; Wu and Gosselin 2007). For a link i with mass m_i and its axial moment of inertia I_i, we have

$$\begin{bmatrix} 1 & 1 & 1 \\ r_i & 0 & 1-r_i \\ r_i^2 L_i^2 & 0 & (1-r_i)^2 L_i^2 \end{bmatrix} \begin{bmatrix} m_{i1} \\ m_{i2} \\ m_{i3} \end{bmatrix} = \begin{bmatrix} m_i \\ 0 \\ I_i \end{bmatrix}, \quad (i = 1, 2, 3, 4), \tag{12}$$

where m_{ij} ($j = 1, 2, 3$) are the values of the three point masses placed at the centers of the revolute joints and at the center of masses of the link i.

In this case, the kinetic energy T can be written as

$$\begin{aligned} T &= \frac{1}{2}(m_{S1}\mathbf{V}_{S1}^2 + m_{S2}\mathbf{V}_{S2}^2 + m_{S3}\mathbf{V}_{S3}^2 \\ &+ m_{S4}\mathbf{V}_{S4}^2 + m_B\mathbf{V}_B^2 + m_C\mathbf{V}_C^2 + m_D\mathbf{V}_D^2), \end{aligned} \tag{13}$$

where $m_{S1} = m_{12}$, $m_{S2} = m_{22}$, $m_{S3} = m_{32}$, $m_{S4} = m_{42}$, $m_B = m_{13} + m_{21}$, $m_C = m_{23} + m_{21}$ and $m_D = m_{33} + m_{41}$. The terms m_{ij} ($i = 1, 2, 3, 4$) are deduced from the relation (12), $\mathbf{V}_{Si}$ is the vector of the linear velocities of the center of masses S_i; $\mathbf{V}_B$, $\mathbf{V}_C$ and $\mathbf{V}_D$ are the vectors of the linear velocities of the corresponding axes.

The input torques can be obtained from (6):

$$\boldsymbol{\tau} = \mathbf{W_b} + \mathbf{J}_{5R}^{\mathrm{T}} \mathbf{W_p} \tag{14}$$

taking into account that for the examined manipulator

$$\mathbf{W_b} = \mathbf{J_B^T F_B} + \mathbf{J_D^T F_D}, \tag{15}$$

where

$$\begin{aligned} \mathbf{J_B} &= \begin{bmatrix} -L_1 \sin q_1 & 0 \\ L_1 \cos q_1 & 0 \end{bmatrix}, \\ \mathbf{J_D} &= \begin{bmatrix} 0 & -L_4 \sin q_2 \\ 0 & L_4 \cos q_2 \end{bmatrix}, \end{aligned} \tag{16}$$

$$\begin{aligned} \mathbf{F_B} &= m_{B1}\boldsymbol{\Gamma_B} + m_{C1}\boldsymbol{\Gamma_C}, \\ \mathbf{F_D} &= m_{D2}\boldsymbol{\Gamma_D} + m_{C3}\boldsymbol{\Gamma_C}, \end{aligned} \tag{17}$$

$$\boldsymbol{\Gamma_B} = L_1 \left(\ddot{q}_1 \begin{bmatrix} -\sin q_1 \\ \cos q_1 \end{bmatrix} - \dot{q}_1^2 \begin{bmatrix} \cos q_1 \\ \sin q_1 \end{bmatrix} \right),$$

$$\mathbf{\Gamma_D} = L_4 \left(\ddot{q}_2 \begin{bmatrix} -\sin q_2 \\ \cos q_2 \end{bmatrix} - \dot{q}_2^2 \begin{bmatrix} \cos q_2 \\ \sin q_2 \end{bmatrix} \right),$$

$$\mathbf{\Gamma_C} = \begin{bmatrix} \ddot{x} \\ \ddot{y} \end{bmatrix}, \tag{18}$$

$$m_{B1} = m_{S1} r_1^2 + m_B + m_{S2}(1 - r_2)^2,$$

$$m_{C1} = m_{S2} r_2 (1 - r_2), \tag{19}$$

$$m_{C3} = m_{S3} r_3 (1 - r_3),$$

$$m_{D2} = m_{S4} r_4^2 + m_D + m_{S3}(1 - r_3)^2. \tag{20}$$

The term $\mathbf{W_p}$ is given by

$$\mathbf{W_p} = m_{C1}\mathbf{\Gamma_B} + m_{C2}\mathbf{\Gamma_C} + m_{C3}\mathbf{\Gamma_D}, \tag{21}$$

$$m_{C2} = m_{S2} r_2^2 + m_C + m_{S3} r_3^2 \tag{22}$$

and the Jacobian matrix $\mathbf{J}_{5R}$ is given by

$$\mathbf{J}_{5R} = \mathbf{A}_{5R}^{-1} \mathbf{B}_{5R}, \tag{23}$$

where

$$\mathbf{A}_{5R} = \begin{bmatrix} a_{11} & a_{12} \\ a_{21} & a_{22} \end{bmatrix} = 2 \begin{bmatrix} x - L_1 \cos q_1 + a & y - L_1 \sin q_1 \\ x - L_4 \cos q_2 - a & y - L_4 \sin q_2 \end{bmatrix}, \tag{24}$$

$$\mathbf{B}_{5R} = - \begin{bmatrix} L_1 \begin{pmatrix} a_{11} \sin q_1 \\ -a_{12} \cos q_1 \end{pmatrix} & 0 \\ 0 & L_4 \begin{pmatrix} a_{21} \sin q_2 \\ -a_{22} \cos q_2 \end{pmatrix} \end{bmatrix}. \tag{25}$$

and we determine $\mathbf{t_s}$ in accordance with (8):

$$\mathbf{t_s} = [-\sin \psi_1, \cos \psi_1]^{\mathrm{T}}. \tag{26}$$

Thus, the examined manipulator can pass through the given singular positions if the wrench $\mathbf{W_p}$ determined by (21) is orthogonal to the direction of the uncontrollable motion $\mathbf{t_s}$ described by (26).

Let us now consider the motion planning, which makes it possible to satisfy this condition. For this purpose the following parameters of the manipulator's links are specified: $L_1 = L_2 = L_3 = L_4 = 0.25$ m; $r_1 = r_2 = r_3 = r_4 = 0.5$; $a = 0.2$ m; $m_1 = m_4 = 2.81$ kg; $I_1 = I_4 = 0.02$ kg/m^2; $m_2 = m_3 = 1.41$ kg; $I_2 = I_3 = 0.01$ kg/m^2.

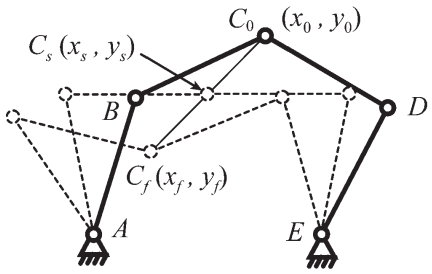

Fig. 3. Initial, singular and final positions of the planar 5R parallel manipulator.

With regard to the prescribed trajectory generation, the point C should reproduce a motion along a straight line between the initial position C_0 $(x_0, y_0) = C_0$ (0.1, 0.345) and the final point C_f $(x_f, y_f) = C_f$ (-0.1, 0.145) in $t_f = 2$ s.

Thus, the given trajectory can be expressed as follows:

$$\mathbf{x} = \begin{bmatrix} x(t) \\ y(t) \end{bmatrix} = \begin{bmatrix} x_0 + s(t)(x_f - x_0) \\ y_0 + s(t)(y_f - y_0) \end{bmatrix}. \tag{27}$$

However, the manipulator will pass through a type 2 singular position at point C_s $(x_s, y_s) = C_s$ (0, 0.245) (Figure 3).

Developing the condition for passing through the singular position (11) for the planar 5R parallel manipulator at point C_s, we obtain

$$m_{C1} L_1 (248\dot{x}^2 - 48\dot{y}^2) - 3\sqrt{6} m_{C2} \ddot{y} = 0. \tag{28}$$

Then, taking into account that the velocity and the acceleration of the end-effector in initial and final positions are equal to zero, the following nine boundary conditions are found:

$$s(t_0) = 0, \tag{29}$$

$$s(t_f) = 1, \tag{30}$$

$$s(t_s = 1s) = 0.5, \tag{31}$$

$$\dot{s}(t_0) = 0, \tag{32}$$

$$\dot{s}(t_f) = 0, \tag{33}$$

$$\dot{s}(t_s) = \dot{y}_s/(y_f - y_0) = \dot{x}_s/(x_f - x_0) = 1, \tag{34}$$

$$\ddot{s}(t_0) = \ddot{s}_0 = 0, \tag{35}$$

$$\ddot{s}(t_f) = \ddot{s}_f = 0, \tag{36}$$

$$\ddot{s}(t_s) = \ddot{s}_s = \frac{m_{C1} L_1 (248\ddot{x}_s^2 - 48\dot{y}_s^2)}{(3(x_f - x_0)\sqrt{6} m_{C2})}. \tag{37}$$

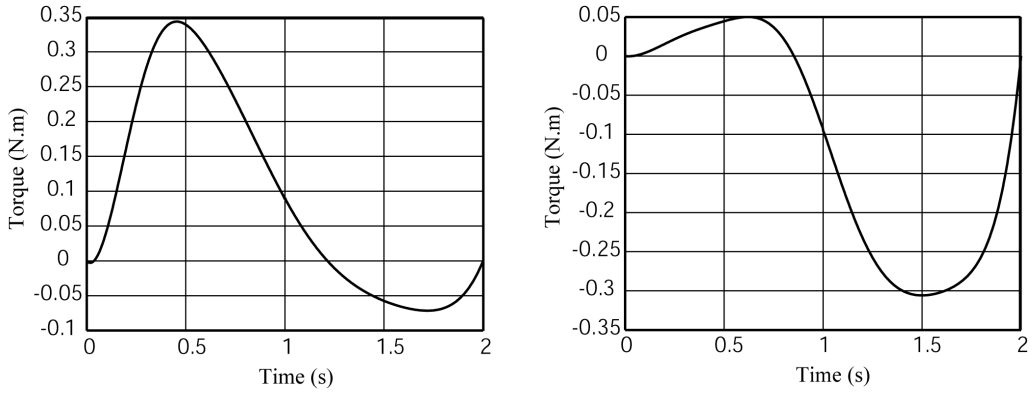

(a) Actuator 1 (b) Actuator 2

Fig. 4. Input torques of the planar 5R parallel manipulator in the case of the eighth-order polynomial trajectory planning, obtained by the ADAMS software.

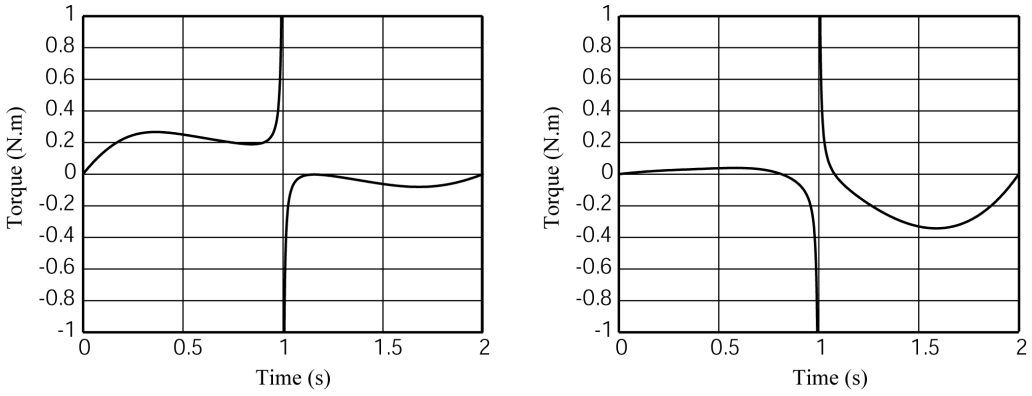

(a) Actuator 1 (b) Actuator 2

Fig. 5. Input torques of the planar 5R parallel manipulator in the case of the fifth-order polynomial trajectory planning, obtained by the ADAMS software.

From (28)–(37), the following eighth-order polynomial trajectory planning is found:

$$s(t) = -0.25851t^3 + 3.84228t^4 - 5.72792t^5 + 3.58909t^6 - 1.07101t^7 + 0.12606t^8. \quad (38)$$

Thus, the generation of the motion by the obtained eighth-order polynomial makes it possible to pass through the singularity without perturbation and the input torques remain in the limits of finite values, which are validated through numerical simulations carried out by the ADAMS software (Figure 4).

Thus, we can assert that the obtained optimal dynamic conditions assume that the manipulator's end-effector passes through the singular position.

Now, we would like to show that, in the case of the generation of the motion by any trajectory planning without meeting the adopted boundary conditions, the end-effector is not able to pass through the singular position. For the purpose of generating motion between the initial and final positions, let us generate a fifth-order polynomial trajectory planning:

$$s(t) = 1.25t^3 - 0.9375t^4 + 0.1875t^5. \quad (39)$$

The obtained numerical simulations carried out by the software ADAMS are given in Figure 5. We can see that, when the manipulator is close to the singular configuration (for $t_s = 1$ s), the values of the input torques tend to infinity.

3.2. Example 2: PAMINSA

The second example we present concerns a parallel manipulator, which was invented and developed at the I.N.S.A of

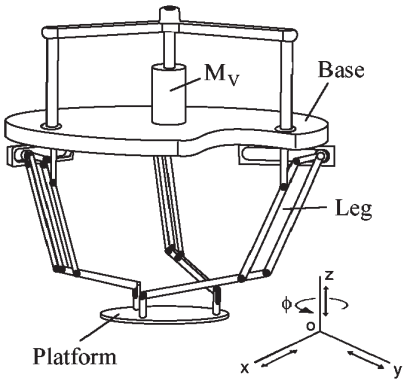

Fig. 6. PAMINSA with four DOF.

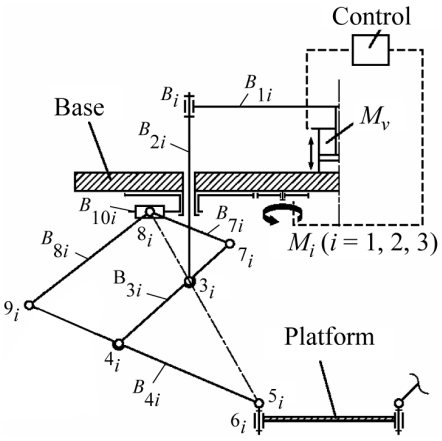

Fig. 7. Kinematic chain of each leg.

Rennes (Arakelian et al. 2006b): PAMINSA (Parallel Manipulator of the I.N.S.A.). The particularity of this architecture is in decoupling of the displacements of the platform in the horizontal plane from the translations along the vertical axis. The advantages of such an approach were disclosed in Arakelian et al. (2005) and Briot et al. (2007b) and the singularity analysis was discussed in Briot et al. (2007a), Briot and Arakelian (2008) and Arakelian et al. (2006a).

The previous studies have revealed that there are type 2 singularities in the workspace of the symmetrical architecture of PAMINSA. Let us illustrate the proposed approach for the PAMINSA with four DOF (Figure 6).

Each leg of this manipulator is realized by a pantograph mechanism (Figure 7) with two input points 3_i and 8_i, and an output point 5_i ($i = 1, 2, 3$). Each input point 8_i is connected to the rotating drive M_i by means of a prismatic guide mounted on a rotating link. This kind of architecture allows for the generation of motion in the horizontal plane by the use of rotating actuators M_1, M_2, M_3, and the vertical translations by means of the linear actuator M_v. Thus, the displacements (x, y, ϕ) of the platform in the horizontal plane ***xOy***, that are translations along the ***x***- and ***y***-axes, and rotations about the ***z***-axis are independent of vertical translations z.

This implies that the kinematic models controlling the displacement of the manipulator can be divided into two parts:

(i) a model for the displacements in the horizontal plane, which is equivalent to a 3-RPR manipulator. R and P stand for passive revolute and prismatic joints, respectively, and R for an actuated revolute joint;

(ii) a model for the translations along the vertical axis equivalent to the model for the vertical translations of a pantograph linkage.

The type 2 singularities of such a manipulator appear when (Arakelian et al. 2006a; Briot et al. 2007a):

(a) the three legs of the manipulators are in parallel, which is impossible for the developed PAMINSA manipulator;

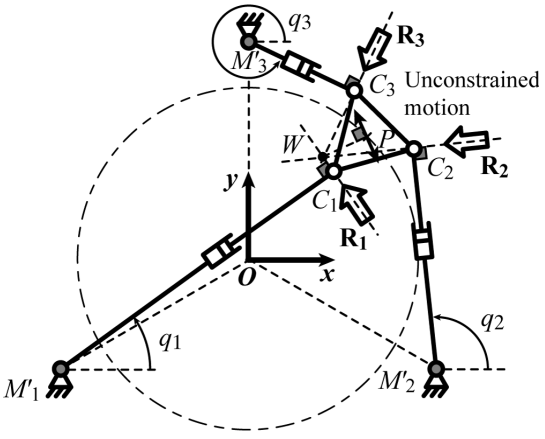

Fig. 8. Example of a type 2 singular configuration (horizontal projection of the examined structure).

(b) the orientation of the platform is equal to $\cos^{-1}(R_{pl}/R_b)$, where R_{pl} and R_b correspond respectively to the lengths PC_i and OM'_i (Figure 8); in this case, the manipulator gains one infinitesimal rotation around one vertical axis;

(c) the platform is located in a circle defined by

$$x^2 + y^2 = R_{pl}^2 + R_b^2 - 2R_{pl}R_b\cos\phi; \qquad (40)$$

in this case, the manipulator gains one finite rotation about one vertical axis (Cardanic self motion) (Briot et al. 2007a).

For cases (b) and (c), the direction of the unconstrained motion can be represented by the twist $\mathbf{t_s} = [0, 0, 1, x_W, y_W, 0]^T$, where x_W and y_W corresponds to the planar coordinates of the intersection point of the wrenches $\mathbf{R}_i$ applied on the platform by the three legs of the manipulator (Figure 8).

Let us now study the inverse dynamics of the PAMINSA. The potential energy V can be written as

$$V = V_{pl} + \sum_{i=1}^{3} V_{leg_i}, \tag{41}$$

where V_{pl} is the potential energy of the platform and V_{leg_i} is the potential energy of the leg i (i = 1, 2, 3).

By further considering that the coordinates of all of the points of the pantograph linkages can be found as a linear combination of the coordinates of points 3_i, 5_i and 9_i, one can express the terms V_{pl} and V_{leg_i} as follows:

$$V_{pl} = m_{pl} g z, \tag{42}$$

$$V_{leg_i} = C_{v1} z_{5i} + C_{v2} z_{9i} + C_{v3} q_v + C_{v4}. \tag{43}$$

Here C_{vj} (j = 1, 2, 3) are constant terms whose dimension is equivalent to a mass multiplied by the gravitational acceleration g, m_{pl} is the mass of the platform with a payload, and z_{5i} and z_{9i} are the altitude of joints 5_i and 9_i. The expressions of the coordinates of joints 5_i and 9_i are given in Appendix A. The expressions for C_{vj} (j = 1, ..., 4) are given in Appendix B.

We consider that the links are perfect tubes. Therefore, the tensor of inertia $\mathbf{I}_j$ of the link B_{ji} at the center of masses will be written as

$$\mathbf{I}_j = \begin{bmatrix} I_{XX}^{(j)} & 0 & 0 \\ 0 & I_{YY}^{(j)} & 0 \\ 0 & 0 & I_{ZZ}^{(j)} \end{bmatrix}, \quad \text{with } I_{YY}^{(j)} = I_{ZZ}^{(j)}. \tag{44}$$

Thus, the kinetic energy T of the manipulator can be represented as

$$T = T_{pl} + \sum_{i=1}^{3} T_{leg_i}, \tag{45}$$

where T_{pl} is the kinetic energy of the platform, T_{legi} is the kinetic energy of the leg i, and

$$T_{pl} = \frac{1}{2}\left(m_{pl}(\dot{x}^2 + \dot{y}^2 + \dot{z}^2) + I_{pl}\dot{\phi}^2\right), \tag{46}$$

where I_{pl} is the axial moment of inertia of the platform about the vertical axis. In addition,

$$T_{leg_i} = T_{trans_i} + T_{rot_i}, \tag{47}$$

$$\begin{aligned} T_{trans_i} &= C_{c1}(\dot{x}_{5i}^2 + \dot{y}_{5i}^2) + C_{c2}\dot{z}_{5i}^2 + C_{c3}(\dot{x}_{9i}^2 + \dot{y}_{9i}^2 + \dot{z}_{9i}^2) \\ &+ C_{c4}(\dot{x}_{5i}\dot{x}_{9i} + \dot{y}_{5i}\dot{y}_{9i}) + C_{c5}\dot{z}_{5i}\dot{z}_{9i} \\ &+ C_{c6}\dot{q}_v^2 + C_{c7}\dot{z}_{5i}\dot{q}_v + C_{c8}\dot{q}_i^2, \end{aligned} \tag{48}$$

where T_{rot_i} is the kinetic energy of the rotating links.

Note that there are two types of rotations (see, Fig. 7):

(i) rotation due to the actuators M_i (i = 1, 2, 3) (angle q_i), which is about the vertical axis;

(ii) rotation due to the displacement of the pantograph in the linkage plane (angles ζ_i and ε_i denoted as the angles between the direction of the passive slider and the links B_{4i} and B_{3i} respectively).

Thus, the kinetic energy of the rotating links can be written as

$$\begin{aligned} T_{rot_i} &= C_{c9}\dot{\zeta}_i^2 + C_{c10}\dot{\varepsilon}_i^2 + \dot{q}_i^2(C_{c13} + C_{c10}\sin^2\varsigma_i \\ &+ C_{c9}\cos^2\varsigma_i + C_{c12}\sin^2\varepsilon_i + C_{c11}\cos^2\varepsilon_i). \end{aligned} \tag{49}$$

The expressions for C_{cj} (j = 1, ..., 13) are given in Appendix C.

The input torques can be obtained from (6):

$$\boldsymbol{\tau} = \mathbf{W_b} + \mathbf{J}_{PAM}^{\mathrm{T}} \mathbf{W_p}, \tag{50}$$

where the terms $\mathbf{J}_{PAM}$, $\mathbf{W_b}$ and $\mathbf{W_p}$ are presented in Appendix D.

The following parameters of manipulator's links are specified for the trajectory generation:

- the radii of the circles circumscribed to the base and platform triangles are respectively equal to R_b = 0.35 m and R_{pl} = 0.1 m;
- the magnification factor of the pantograph, k = 3;
- gravitational acceleration g is equal to 9.81 m/s^2;
- the lengths of the links of the pantograph linkages, L_{B1} = 0.308 m, L_{B2} = 0.442 m, L_{B3} = L_{B8} = 0.42 m, L_{B4} =k L_{B7} = 0.63 m, L_{B5} = 0.0275 m, L_{B10} = 0.3635 m;
- the masses of the joints of the pantograph linkages, m_2 = 0.214 kg, m_3 = 0.338 kg, m_4 = 0.262 kg, m_5 = 0.233 kg, m_7 = 3.08 kg, m_8 = 0.305 kg, m_9 = 0.259 kg;
- the mass of the platform, m_{pl} = 2.301 kg;
- the masses of the links of the pantograph linkages, m_{B1} =1.221 kg, m_{B2} = 0.921 kg, m_{B3} = 0.406 kg, m_{B4} = 0.672 kg, m_{B7} = 0.107 kg, m_{B8} = 0.403 kg, m_{B10} = 0.436 kg;
- the term of the inertia matrix of the platform, I_{pl} = 0.015kg.m^2;
- the terms of the inertia matrices of the links of the pantograph linkages, $I_{XX}^{(B3)}$ = 0.0038kg.m^2, $I_{YY}^{(B3)}$ = 0.02kg.m^2, $I_{XX}^{(B4)}$ = 0.0012kg.m^2, $I_{YY}^{(B4)}$ = 0.048kg.m^2, $I_{XX}^{(B7)}$ = $8 \cdot 10^{-4}$kg.m^2, $I_{YY}^{(B7)}$ = 0.003kg.m^2, $I_{XX}^{(B8)}$ = 0.0024kg.m^2, $I_{YY}^{(B8)}$ = 0.02kg.m^2, I_{B2} = 0.003kg.m^2, I_{B10} = 0.02kg.m^2.

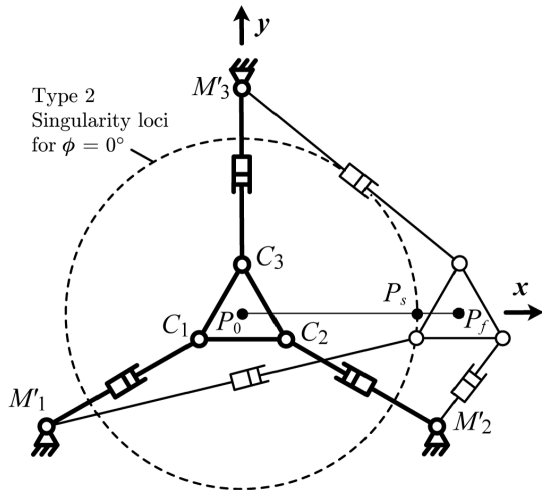

Fig. 9. Displacement of the PAMINSA along the prescribed straight line (planar projection).

The point P is desired to make a motion $x(t)$ along a straight line between points P_0 $(x_0, y_0) = P_0$ (0, 0) and point P_f $(x_f, y_f) = P_f$ (0.3, 0) in $t_f = 2.4$ s. However, the manipulator will pass through a type 2 singular position at point P_s $(x_s, y_s) =$ (0.25, 0) (Figure 9).

In order to carry out a comparative analysis for the optimized and non-optimized dynamic conditions for passing through type 2 singularity, we consider two cases. The first is such a movement on the given trajectory, which is calculated from condition (11), and the second is an arbitrary motion.

First let us consider an optimized trajectory which allows the condition (11) to be satisfied, that is, the force $\mathbf{W_p}$ should be perpendicular to the twist $\mathbf{t_s}$ $[0, 0, 1, 0, 0.1, 0]^{\mathrm{T}}$ defining the direction of the unconstrained motion. Developing the expression (11) for the PAMINSA at point P_s, we obtain

$$\begin{aligned} 0 &= 0.06441\ddot{x} + 1.2115\ddot{y} - 0.14649\ddot{z} + 0.04425\ddot{\phi} \\ &+ 0.06827 + 6.85084\dot{x}^2 + 0.11720\dot{y}^2 - 0.18482\dot{z}^2 \\ &+ 0.02947\dot{\phi}^2 - 0.85175\dot{\phi}\dot{x} + 0.05643\dot{\phi}\dot{y} + 0.19423\dot{\phi}\dot{z} \\ &- 5.17625\dot{x}\dot{y} + 0.46477\dot{x}\dot{z} + 2.94694\dot{y}\dot{z}. \end{aligned} \quad (51)$$

Now considering that the end-effector of the manipulator moves along a straight line directed along the $\boldsymbol{x}$-axis, we can note that $\dot{y}(t_s) = \dot{z}(t_s) = \ddot{y}(t_s) = \ddot{z}(t_s) = \dot{\phi}(t_s) = \ddot{\phi}(t_s) = 0$. Thus, the relationships that satisfy the condition of passing through the singular positions, taking into account that the velocity and the acceleration of the platform in the initial and final positions are equal to zero, can be expressed by the following boundary conditions:

$$x(t_0) = x_0, \quad (52)$$

$$x(t_f) = x_f, \quad (53)$$

$$x(t_s = 2s) = x_s, \quad (54)$$

$$\dot{x}(t_0) = 0, \quad (55)$$

$$\dot{x}(t_f) = 0, \quad (56)$$

$$\ddot{x}(t_0) = 0, \quad (57)$$

$$\ddot{x}(t_f) = 0, \quad (58)$$

$$\dot{x}(t_s) = \dot{x}_s = 0.05 \text{ m/s}, \quad (59)$$

$$\ddot{x}(t_s) = \ddot{x}_s = -1.32583 \text{ m/s}^2. \quad (60)$$

In this case, a motion for the passing of the platform through the singular position can be found from the following eighth-order polynomial form:

$$\begin{aligned} x(t) &= 3.41t^8 - 37.65t^7 + 166.05t^6 - 365.23t^5 \\ &+ 400.63t^4 - 175.27t^3. \end{aligned} \quad (61)$$

However, a trajectory obtained by (61) cannot be reproduced by the prototype because of the limited capability of the drivers' deceleration. Therefore, the trajectory was divided into two parts, that is, the first sixth-order polynomial trajectory assumes the motion from an initial to the singular position (P_0P_s) and the second sixth-order polynomial trajectory from singular to the final position (P_sP_f). The core of the problem is the same but it allows for motions to be generated for the prototype.

Thus, the trajectory planning equations can be written as

$$\begin{aligned} x(t) &= x_0 + (x_s - x_0) \\ &\times \left(b_3t^3 + b_4t^4 + b_5t^5 + b_6t^6\right) \quad \text{for } t \le t_s, \end{aligned} \quad (62)$$

$$\begin{aligned} x(t) &= x_s + \left(x_f - x_s\right)\left(c_1(t - t_s) + c_2(t - t_s)^2 + c_4(t - t_s)^4\right. \\ &+ \left. c_5(t - t_s)^5 + c_6(t - t_s)^6\right) \quad \text{for } t > t_s. \end{aligned} \quad (63)$$

with $b_3 = -3.3033$, $b_4 = 5.10456$, $b_5 = -2.45207$, $b_6 = 0.37844$, $c_1 = 1$, $c_2 = -13.25829$, $c_4 = 2{,}365.3672$, $c_5 = -11{,}953.07236$ and $c_6 = 16{,}158.76157$.

Thus, the motion obtained from the following sixth-order polynomial equations:

$$\begin{aligned} x(t) &= -0.826t^3 + 1.276t^4 - 0.613t^5 + 0.095t^6 \\ \text{for } t &\le 2s, \end{aligned} \quad (64)$$

$$\begin{aligned} x(t) &= 72722.7 - 206718.3t + 244555.2t^2 - 154122.4t^3 \\ &+ 54571.1t^4 - 10292.9t^5 + 807.9t^6 \quad \text{for } t > 2s, \end{aligned} \quad (65)$$

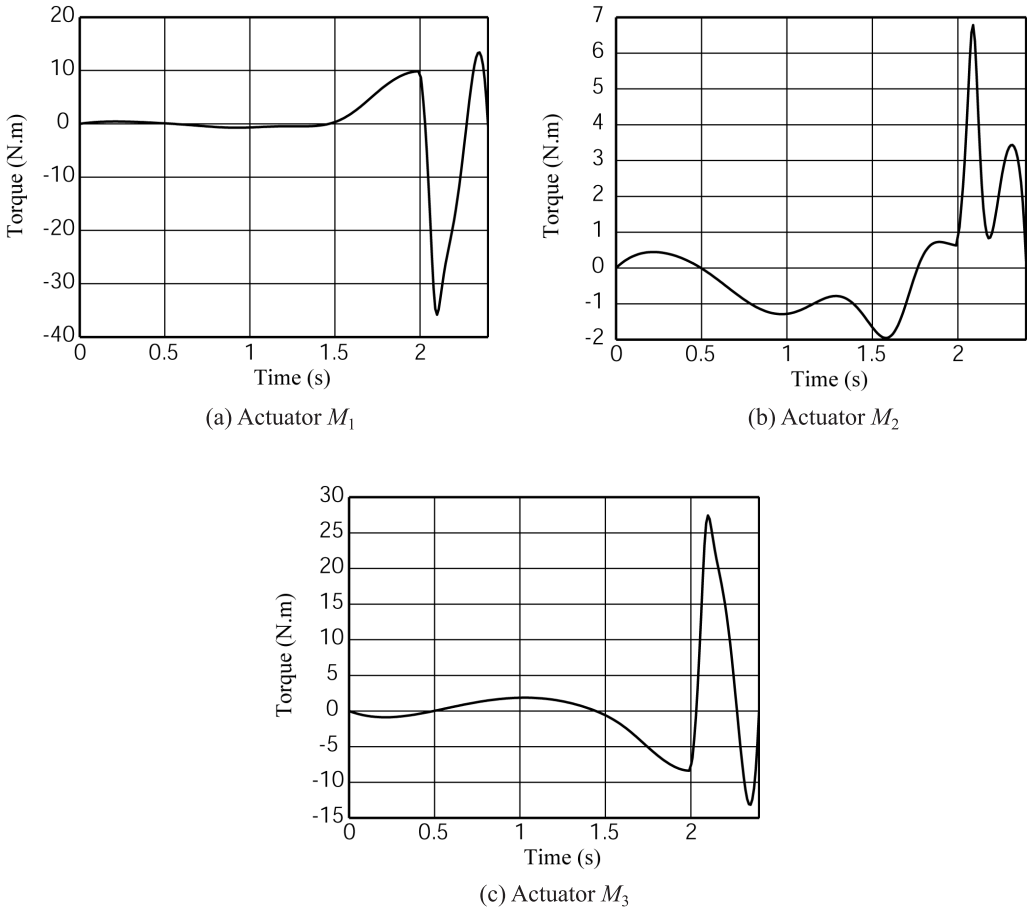

Fig. 10. Input efforts of the PAMINSA in the case of the sixth-order polynomial trajectory planning, computed using the ADAMS software.

which allows the singularity to be passed through without perturbation, and the input efforts take on finite values (Figure 10).

It can be seen that the input torques remain in the limits of finite values, but, by the end of the motion, there is an increase of the input efforts, caused by a quick deceleration to stop the manipulator before it reaches the workspace boundary. We further show below that in the case of the motion generated by any trajectory planning without meeting the adopted boundary conditions (52)–(60), the manipulator platform is not able to pass through the singular position. For this purpose, the generation of motion between the initial and final positions is carried out by a fifth-order polynomial trajectory planning.

In this case, for $y(t) = 0$ m, $z(t) = -0.45$ m and $\phi(t) = 0$, the fifth-order polynomial trajectory planning is as follows:

$$x(t) = 0.217t^3 - 0.137t^4 + 0.023t^5. \quad (66)$$

The obtained input efforts computed by the software ADAMS are represented in Figure 11.

It should be noted that, while the manipulator passes through the singular configuration (for $t_s \approx 1.8$ s), the values of the input torques tend to infinity.

Let us now validate the results obtained using experimental tests.

4. Experimental Validation of the Obtained Results

To validate the results of the previous section, we have carried out experimental tests on the prototype of the PAMINSA developed in the I.N.S.A. of Rennes (Figure 12).

First, we applied an arbitrary fifth-order control law and observed the reproduction of motion during the displacement of the platform. The obtained trajectory is shown in Figure 13 (dotted line).

The different positions are classified by time. For positions (a) to (d), the platform moves towards the singular zone but

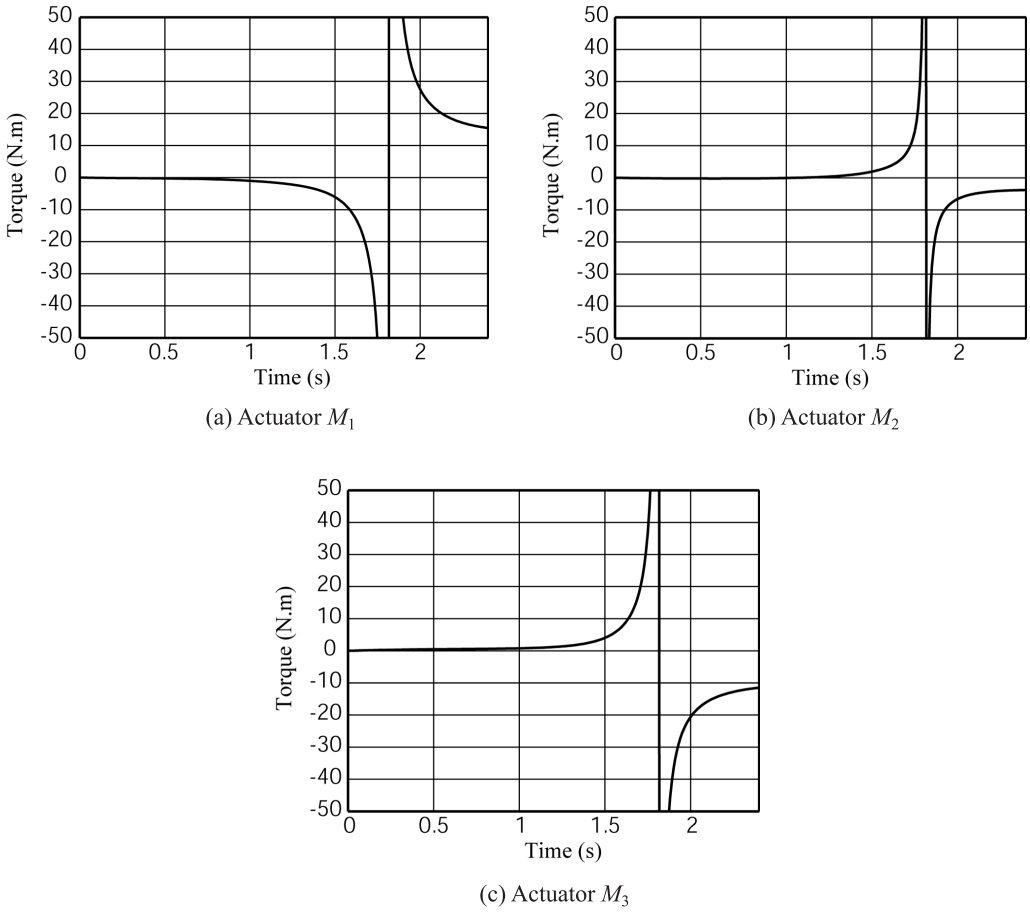

(a) Actuator M_1

(b) Actuator M_2

(c) Actuator M_3

Fig. 11. Input efforts of the PAMINSA in the case of the fifth-order polynomial trajectory planning, computed using the ADAMS software.

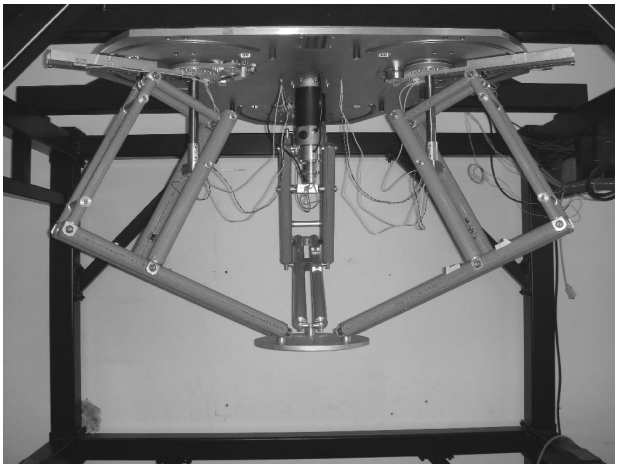

Fig. 12. The prototype of PAMINSA developed in the I.N.S.A. of Rennes.

it remains outside of it. In this case, the reproduction of the real trajectory is similar to the desirable. At position (e), the manipulator enters the singular zone, which is close to the circle of the theoretical singular loci, and starts an uncontrollable motion. Thus, since the motion generation is carried out by non-optimized dynamic parameters, the platform moves along an unplanned trajectory (see positions (e)–(h) in Figure 13).

Next, we implemented the sixth-order control law as shown in the previous section and observed the behavior of the platform during the displacement (Figure 14). The different positions are classified by time. During all of these displacements, the manipulator retains its orientation and passes through the singular configuration without any perturbation.

Thus, we can note that the obtained optimum dynamic conditions allow the manipulator to pass through the singular position.

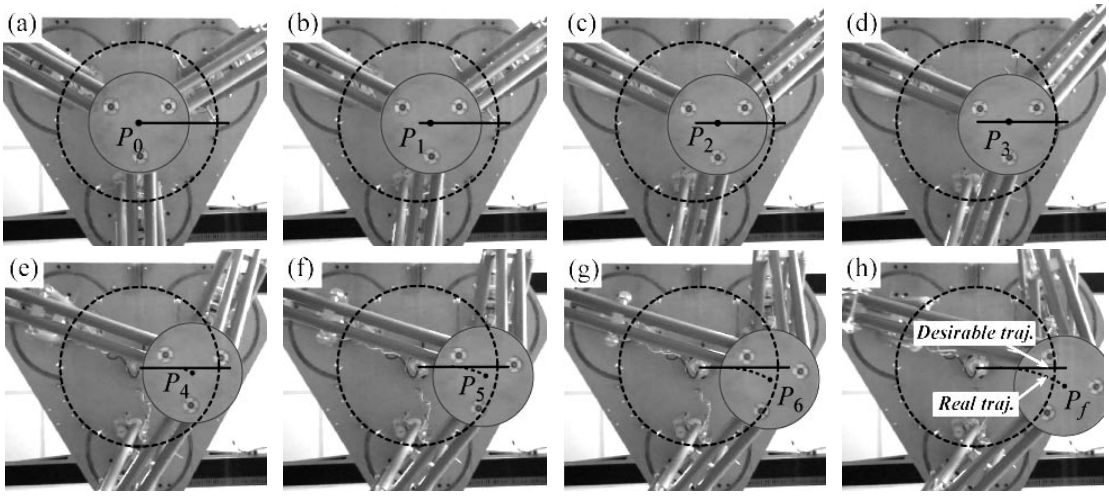

Fig. 13. Trajectory reproduction on the PAMINSA during the displacement of the platform with the fifth-order polynomial law (view from below).

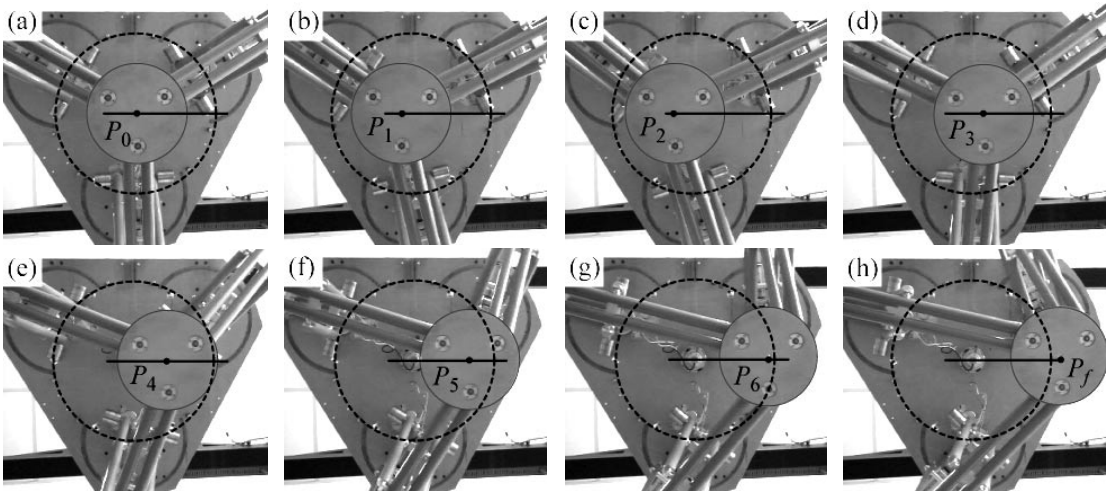

Fig. 14. Trajectory reproduction on the PAMINSA during the displacement of the platform with the sixth-order polynomial law (view from below).

5. Conclusion

At a singular configuration, a manipulator can gain one or more DOF, and at such a configuration it may become uncontrollable, that is, it may not reproduce stable motion with a prescribed trajectory. Nevertheless, there are several motion planning techniques that allow these singular zones to be passed through. These approaches have simulated by numerical examples and illustrated on several parallel structures. It is a promising tendency for the solution of this problem. However, attention has focused only on control aspects of this problem and very little attention has been paid to the dynamic interpretation, which is a crucial factor for governing the behavior of parallel manipulators at the singular zones.

In this paper we have found the optimal dynamic conditions to make passing through the type 2 singular configurations possible. The general definition of the condition for passing through the singular position is formulated as follows: in the presence of type 2 singular configuration, the platform of a parallel manipulator can pass through the singular positions without perturbation of motion if the wrench applied on the platform by the legs and external efforts are orthogonal to the direction of the uncontrollable motion or, in other words, if the work of the applied forces and moments on the platform along

the uncontrollable motion is equal to zero. This condition has been verified by numerical simulations carried out with the software ADAMS and validated by experimental tests on the prototype four-DOF parallel manipulator PAMINSA.

It should be noted that the formulated general conditions should apply to any given trajectory generation through Type 2 singular configurations in the manipulator workspace. We would like to point out that the trajectory is not imposed and only the conditions of force generation must be satisfied.

Thus, the passing of any parallel manipulator through the singular positions by the proposed technique is carried out by the optimal generation of inertia forces. Hence, it is impossible to stop the manipulator in the singular locus and to start again from a fixed position.

We would like to mention that we have studied the optimal redistribution of forces only in singular positions of the manipulator, but it should be noted that there are zones close to these positions in which the manipulator loses the quality of motion. For a more reliable generation of motion, it is desirable to ensure the given condition of force generation not only in the singular positions of the manipulator but also in the zones near to these positions. It should also be mentioned that a future development of our work will involve studying the difficulties of controlling parallel robots in the neighborhood of singular configurations.

Finally, it should be noted that the proposed technique cannot be used for the case of non-controllable external forces applied on the platform. Therefore, the most prominent field of the industrial application is a "fast pick and place" manipulation, when the generation of motion is determined by input, gravitational and inertia forces.

Appendix A

The coordinates of points 3_i, 5_i and 9_i ($i = 1, 2, 3$) are

$$\begin{bmatrix} x_{3i} \\ y_{3i} \\ z_{3i} \end{bmatrix} = \begin{bmatrix} R_b \cos\gamma_i \\ R_b \sin\gamma_i \\ z_{5i}/k \end{bmatrix},$$

$$\begin{bmatrix} x_{5i} \\ y_{5i} \\ z_{5i} \end{bmatrix} = \begin{bmatrix} x \\ y \\ z \end{bmatrix} + \begin{bmatrix} R_{pl}\cos(\phi+\gamma_i) \\ R_{pl}\sin(\phi+\gamma_i) \\ L_c \end{bmatrix},$$

where $\gamma_i = (-5\pi/6, -\pi/6, \pi/2)$,

$$\begin{bmatrix} x_{9i} \\ y_{9i} \\ z_{9i} \end{bmatrix} = \begin{bmatrix} x_{3i} + X_{9i}\cos q_i \\ y_{3i} + X_{9i}\sin q_i \\ F \end{bmatrix},$$

with

$$\begin{aligned}
X_{9i} &= A + BF, \quad F = -(D-K)/(2E),\\
K &= \sqrt{D^2 - 4EC}, \quad E = -(B^2+1),\\
D &= 2B(X_{8i} - A), \quad C = L_{B3}^2 - X_{8i}^2 + 2AX_{8i} - A^2,\\
B &= z_{5i}/(kX_{8i}),\\
A &= (L_{B4}^2 - L_{B3}^2 - X_{5i}^2 + X_{8i}^2 - z_{5i}^2)/(2kX_{8i}),\\
X_{8i} &= -X_{5i}/(k-1),\\
X_{5i} &= \sqrt{(x_{5i}-x_{3i})^2 + (y_{5i}-y_{3i})^2}.
\end{aligned}$$

Appendix B

The expressions of terms C_{vj} ($j = 1, \ldots, 4$) are

$$\begin{aligned}
C_{v1} &= g\left(m_5 + \sum_{j=2,3,4,7}\left(\frac{m_j}{k}\right) + \frac{m_{B4}}{2}\right.\\
&\quad \left. + \sum_{j=1,7}\left(\frac{m_{Bj}}{2k}\right) + \sum_{j=2}^{3}\left(\frac{m_{Bj}}{k}\right)\right),\\
C_{v2} &= g\left(\frac{(k-1)m_4 - m_7 + km_9}{k}\right.\\
&\quad \left. + \frac{(k-2)m_{B3} - m_{B7}}{2k} + \frac{m_{B4}+m_{B8}}{2}\right),\\
C_{v3} &= g\frac{m_{B1}}{2}, \quad C_{v4} = gL_{B2}\left(m_2 + \frac{m_{B1}+m_{B2}}{2}\right).
\end{aligned}$$

Appendix C

The expressions of terms C_{cj} ($j = 1, \ldots, 13$) are

$$\begin{aligned}
C_{c1} &= \frac{1}{2}\left(\frac{m_4}{k^2} + m_5 + \frac{m_7}{(k(k-1))^2} + \frac{m_8}{(k-1)^2}\right.\\
&\quad + \frac{m_{B3}(k-2)^2}{(2k(k-1))^2} + \frac{m_{B4}}{4} + \frac{m_{B7}(k+1)^2}{(2k(k-1))^2}\\
&\quad \left. + \frac{m_{B8}}{(2(k-1))^2}\right),\\
C_{c2} &= \frac{1}{2}\left(\sum_{j=2,3,4,7}\left(\frac{m_j}{k^2}\right) + m_5 + \sum_{j=1,7}\left(\frac{m_{Bj}}{4k^2}\right)\right.\\
&\quad \left. + \sum_{j=2}^{3}\left(\frac{m_{Bj}}{k^2}\right) + \frac{m_{B4}}{4}\right),
\end{aligned}$$

$$
\begin{aligned}
C_{c3} &= \frac{1}{2}\left(\frac{(k-1)^2 m_4}{k^2} + \frac{m_7}{k^2} + m_9 + \frac{m_{B3}(k-2)^2}{4k^2}\right.\\
&\quad \left. + \frac{m_{B4}}{4} + \frac{m_{B7}}{4k^2} + \frac{m_{B8}}{4}\right),\\
C_{c4} &= \frac{1}{2}\left(\frac{2(k-1)m_4}{k^2} + \frac{m_7}{k^2(k-1)} + \frac{m_{B3}(k-2)^2}{2k^2(k-1)}\right.\\
&\quad \left. + \frac{m_{B4}}{2} + \frac{m_{B7}(k+1)}{2k^2(k-1)} - \frac{m_{B8}}{2(k-1)}\right),\\
C_{c5} &= \frac{1}{2}\left(\frac{4((k-1)m_4 - m_7) - m_{B7} + 2m_{B3}(k-2)}{2k^2} + \frac{m_{B4}}{2}\right),\\
C_{c6} &= \frac{m_{B1}}{8}, \quad C_{c7} = \frac{m_{B1}}{4k}, \quad C_{c8} = \frac{m_{B10} L_{B10}^2}{8},\\
C_{c9} &= \frac{I_{YY}^{(B4)} + I_{YY}^{(B7)}}{2}, \quad C_{c10} = \frac{I_{XX}^{(B4)} + I_{XX}^{(B7)}}{2},\\
C_{c11} &= \frac{I_{YY}^{(B3)} + I_{YY}^{(B8)}}{2}, \quad C_{c12} = \frac{I_{XX}^{(B3)} + I_{XX}^{(B8)}}{2},\\
C_{c13} &= \frac{I_{B2} + I_{B10}}{2}.
\end{aligned}
$$

Appendix D

The global Jacobian matrix is $\mathbf{J}_{PAM} = \mathbf{A}^{-1}\mathbf{B}$ where matrices $\mathbf{A}$ and $\mathbf{B}$ are

$$
\mathbf{A} = -\begin{bmatrix}
\sin q_1 & -\cos q_1 & 0 & -z_{PC1}\cos q_1 & -z_{PC1}\sin q_1 & -\mathbf{PC}_1^{\mathrm{T}}\mathbf{d_1}\\
\sin q_2 & -\cos q_2 & 0 & -z_{PC2}\cos q_2 & -z_{PC2}\sin q_2 & -\mathbf{PC}_2^{\mathrm{T}}\mathbf{d_2}\\
\sin q_3 & -\cos q_3 & 0 & -z_{PC3}\cos q_3 & -z_{PC3}\sin q_3 & -\mathbf{PC}_3^{\mathrm{T}}\mathbf{d_3}\\
0 & 0 & -1 & y_{PC1} & -x_{PC1} & 0\\
0 & 0 & -1 & y_{PC2} & -x_{PC2} & 0\\
0 & 0 & -1 & y_{PC3} & -x_{PC3} & 0
\end{bmatrix},
$$

$$
\mathbf{B} = \begin{bmatrix}
\rho_1 & 0 & 0 & 0\\
0 & \rho_2 & 0 & 0\\
0 & 0 & \rho_3 & 0\\
0 & 0 & 0 & k\\
0 & 0 & 0 & k\\
0 & 0 & 0 & k
\end{bmatrix}
$$

with $\rho_i = \sqrt{(x_{5i}-x_{3i})^2 + (y_{5i}-y_{3i})^2}$, $\mathbf{PC_i} = \left[x_{PCi}, y_{PCi}, z_{PCi}\right]^{\mathrm{T}} = \left[x_{5i}-x, y_{5i}-y, z_{5i}-z\right]^{\mathrm{T}}$ and $\mathbf{d}_i = \begin{bmatrix}\cos q_i & \sin q_i & 0\end{bmatrix}^{\mathrm{T}}$ (for $i = 1, 2, 3$).

The expressions of the terms $\mathbf{W_b}$ and $\mathbf{W_p}$ are

$$
\begin{aligned}
\mathbf{W_b} &= \sum_{i=1}^{3}(\mathbf{J}_{\mathbf{Q}3i}^{\mathrm{T}}\mathbf{F}_{3i} + \mathbf{J}_{\mathbf{Q}4i}^{\mathrm{T}}\mathbf{F}_{4i} + \mathbf{J}_{\mathbf{Q}9i}^{\mathrm{T}}\mathbf{F}_{9i} + \mathbf{J}_{\mathbf{Q}7i}^{\mathrm{T}}\mathbf{F}_{7i}\\
&\quad + \mathbf{J}_{\mathbf{Q}2i}^{\mathrm{T}}\mathbf{F}_{2i} + \mathbf{J}_{\mathbf{Q}S4i}^{\mathrm{T}}\mathbf{F}_{S4i} + \mathbf{J}_{\mathbf{Q}S3i}^{\mathrm{T}}\mathbf{F}_{S3i} + \mathbf{J}_{\mathbf{Q}S8i}^{\mathrm{T}}\mathbf{F}_{S8i}\\
&\quad + \mathbf{J}_{\mathbf{Q}S7i}^{\mathrm{T}}\mathbf{F}_{S7i} + \mathbf{J}_{\mathbf{Q}S10i}^{\mathrm{T}}\mathbf{F}_{S10i} + \mathbf{J}_{\mathbf{Q}S2i}^{\mathrm{T}}\mathbf{F}_{S2i})\\
\mathbf{W_p} &= \mathbf{F_P} + \sum_{i=1}^{3}(\mathbf{J}_{\mathbf{X}8i}^{\mathrm{T}}\mathbf{F}_{8i} + \mathbf{J}_{\mathbf{X}5i}^{\mathrm{T}}\mathbf{F}_{5i} + \mathbf{J}_{\mathbf{X}9i}^{\mathrm{T}}\mathbf{F}_{9i} + \mathbf{J}_{\mathbf{X}4i}^{\mathrm{T}}\mathbf{F}_{4i}\\
&\quad + \mathbf{J}_{\mathbf{X}7i}^{\mathrm{T}}\mathbf{F}_{7i} + \mathbf{J}_{\mathbf{X}S4i}^{\mathrm{T}}\mathbf{F}_{S4i} + \mathbf{J}_{\mathbf{X}S3i}^{\mathrm{T}}\mathbf{F}_{S3i} + \mathbf{J}_{\mathbf{X}S8i}^{\mathrm{T}}\mathbf{F}_{S8i}\\
&\quad + \mathbf{J}_{\mathbf{X}S7i}^{\mathrm{T}}\mathbf{F}_{S7i})
\end{aligned}
$$

with

$$
\mathbf{J}_{\mathbf{X}5i} = \begin{bmatrix}
\left(\frac{\partial[x_{5i}, y_{5i}, z_{5i}]^{\mathrm{T}}}{\partial[x,y,z]^{\mathrm{T}}}\right)_{3\times3} & \mathbf{0}_{3\times3} & \left(\frac{\partial[x_{5i}, y_{5i}, z_{5i}]^{\mathrm{T}}}{\partial\phi}\right)_{3\times1}\\
\mathbf{0}_{3\times3} & \mathbf{0}_{3\times3} & \mathbf{0}_{3\times1}
\end{bmatrix},
$$

$$
\mathbf{J}_{\mathbf{X}8i} = \frac{1}{1-k}\begin{bmatrix}
1 & 0 & \mathbf{0_{1\times4}}\\
0 & 1 & \mathbf{0_{1\times4}}\\
\mathbf{0_{4\times1}} & \mathbf{0_{4\times1}} & \mathbf{0_{4\times4}}
\end{bmatrix}\mathbf{J}_{\mathbf{X}5i},
$$

$$
\mathbf{J}_{\mathbf{Q}3i} = \begin{bmatrix}
\mathbf{0_{2\times3}} & \mathbf{0_{2\times1}}\\
\mathbf{0_{1\times3}} & 1\\
\mathbf{0_{3\times3}} & \mathbf{0_{3\times1}}
\end{bmatrix}, \quad \mathbf{J}_{\mathbf{Q}2i} = \mathbf{J}_{\mathbf{Q}3i},
$$

$$
\mathbf{J}_{\mathbf{Q}9i} = \begin{bmatrix}
\mathbf{0_{1\times3}} & \delta_{1i}\left(\mathbf{R}_{\mathbf{P}qi}\mathbf{Rot}(\varepsilon_i, \mathbf{y})\begin{bmatrix}L_{B3}\\ \mathbf{0_{2\times1}}\end{bmatrix}\right)^{\mathrm{T}}\\
\mathbf{0_{1\times3}} & \delta_{2i}\left(\mathbf{R}_{\mathbf{P}qi}\mathbf{Rot}(\varepsilon_i, \mathbf{y})\begin{bmatrix}L_{B3}\\ \mathbf{0_{2\times1}}\end{bmatrix}\right)^{\mathrm{T}}\\
\mathbf{0_{1\times3}} & \delta_{3i}\left(\mathbf{R}_{\mathbf{P}qi}\mathbf{Rot}(\varepsilon_i, \mathbf{y})\begin{bmatrix}L_{B3}\\ \mathbf{0_{2\times1}}\end{bmatrix}\right)^{\mathrm{T}}\\
\mathbf{0_{1\times3}} & \mathbf{0_{1\times3}}
\end{bmatrix}^{\mathrm{T}},
$$

$$\mathbf{R}_{\mathbf{P}qi} = \begin{bmatrix} -\sin q_i & -\cos q_i & 0 \\ \cos q_i & -\sin q_i & 0 \\ 0 & 0 & 0 \end{bmatrix},$$

$$\mathbf{J}_{X9i} = \begin{bmatrix} \mathbf{Rot}(q_i, \mathbf{z})\mathbf{R}_{\mathbf{P}\varepsilon i} \begin{bmatrix} L_{B3} \\ \mathbf{0_{2\times1}} \end{bmatrix} & \mathbf{0_{3\times1}} \\ \mathbf{0_{3\times1}} & \mathbf{0_{3\times1}} \end{bmatrix} \mathbf{J}_{\mathbf{X}\zeta i\varepsilon i} + \mathbf{J}_{\mathbf{X}8i},$$

$$\mathbf{R}_{\mathbf{P}\varepsilon i} = \begin{bmatrix} -\sin\varepsilon_i & 0 & \cos\varepsilon_i \\ 0 & 0 & 0 \\ -\cos\varepsilon_i & 0 & -\sin\varepsilon_i \end{bmatrix},$$

$$\mathbf{J}_{\mathbf{X}\zeta i\varepsilon i} = -\begin{bmatrix} L_{B3}\sin\varepsilon_i & L_{B4}\sin\zeta_i \\ L_{B3}\cos\varepsilon_i & L_{B4}\cos\zeta_i \end{bmatrix}^{-1} \times \begin{bmatrix} \frac{k}{k-1}\mathbf{J}_{\mathbf{X}\rho i} \\ \begin{bmatrix} \mathbf{0_{1\times2}} & 1 & \mathbf{0_{1\times3}} \end{bmatrix} \mathbf{J}_{\mathbf{X}5i} \end{bmatrix},$$

$$\mathbf{J}_{\mathbf{X}\rho i} = \begin{bmatrix} \frac{\partial\rho_i}{\partial x} & \frac{\partial\rho_i}{\partial y} & \frac{\partial\rho_i}{\partial z} & 0 & 0 & \frac{\partial\rho_i}{\partial\phi} \end{bmatrix},$$

$$\mathbf{J}_{\mathbf{Q}4i} = \begin{bmatrix} \mathbf{0_{1\times3}} & \delta_{1i}\left(\mathbf{R}_{\mathbf{P}qi}\mathbf{Rot}(\zeta_i, \mathbf{y}) \begin{bmatrix} L_{B4}/k \\ \mathbf{0_{2\times1}} \end{bmatrix}\right)^{\mathrm{T}} \\ \mathbf{0_{1\times3}} & \delta_{2i}\left(\mathbf{R}_{\mathbf{P}qi}\mathbf{Rot}(\zeta_i, \mathbf{y}) \begin{bmatrix} L_{B4}/k \\ \mathbf{0_{2\times1}} \end{bmatrix}\right)^{\mathrm{T}} \\ \mathbf{0_{1\times3}} & \delta_{3i}\left(\mathbf{R}_{\mathbf{P}qi}\mathbf{Rot}(\zeta_i, \mathbf{y}) \begin{bmatrix} L_{B4}/k \\ \mathbf{0_{2\times1}} \end{bmatrix}\right)^{\mathrm{T}} \\ \mathbf{0_{1\times3}} & \mathbf{0_{1\times3}} \end{bmatrix}^{\mathrm{T}} + \mathbf{J}_{\mathbf{Q}9i},$$

$$\mathbf{J}_{\mathbf{X}4i} = \begin{bmatrix} \mathbf{0_{3\times1}} & \mathbf{Rot}(q_i, \mathbf{z})\mathbf{R}_{\mathbf{P}\zeta i} \begin{bmatrix} L_{B4}/k \\ \mathbf{0_{2\times1}} \end{bmatrix} \\ \mathbf{0_{3\times1}} & \mathbf{0_{3\times1}} \end{bmatrix} \mathbf{J}_{\mathbf{X}\zeta i\varepsilon i} + \mathbf{J}_{\mathbf{X}9i},$$

$$\mathbf{R}_{\mathbf{P}\zeta i} = \begin{bmatrix} -\sin\zeta i & 0 & \cos\zeta i \\ 0 & 0 & 0 \\ -\cos\zeta i & 0 & -\sin\zeta i \end{bmatrix},$$

$$\mathbf{J}_{\mathbf{Q}7i} = \begin{bmatrix} \mathbf{0_{1\times3}} & \delta_{1i}\left(\mathbf{R}_{\mathbf{P}qi}\mathbf{Rot}(\zeta_i, \mathbf{y}) \begin{bmatrix} L_{B4}/k \\ \mathbf{0_{2\times1}} \end{bmatrix}\right)^{\mathrm{T}} \\ \mathbf{0_{1\times3}} & \delta_{2i}\left(\mathbf{R}_{\mathbf{P}qi}\mathbf{Rot}(\zeta_i, \mathbf{y}) \begin{bmatrix} L_{B4}/k \\ \mathbf{0_{2\times1}} \end{bmatrix}\right)^{\mathrm{T}} \\ \mathbf{0_{1\times3}} & \delta_{3i}\left(\mathbf{R}_{\mathbf{P}qi}\mathbf{Rot}(\zeta_i, \mathbf{y}) \begin{bmatrix} L_{B4}/k \\ \mathbf{0_{2\times1}} \end{bmatrix}\right)^{\mathrm{T}} \\ \mathbf{0_{1\times3}} & \mathbf{0_{1\times3}} \end{bmatrix}^{\mathrm{T}},$$

$$\mathbf{J}_{\mathbf{X}7i} = \begin{bmatrix} \mathbf{0_{3\times1}} & \mathbf{Rot}(q_i, \mathbf{z})\mathbf{R}_{\mathbf{P}\zeta i} \begin{bmatrix} L_{B4}/k \\ \mathbf{0_{2\times1}} \end{bmatrix} \\ \mathbf{0_{3\times1}} & \mathbf{0_{3\times1}} \end{bmatrix} \mathbf{J}_{\mathbf{X}\zeta i\varepsilon i} + \mathbf{J}_{\mathbf{X}8i},$$

$$\mathbf{J}_{\mathbf{Q}S4i} = 0.5\left(\mathbf{J}_{\mathbf{Q}5i} + \mathbf{J}_{\mathbf{Q}9i}\right) + \begin{bmatrix} \mathbf{0_{3\times4}} \\ \mathbf{J}_{\mathbf{Q}\Omega1i} \end{bmatrix},$$

$$\mathbf{J}_{\mathbf{Q}\Omega1i} = \begin{bmatrix} \mathbf{0_{2\times1}} & \mathbf{0_{2\times1}} & \mathbf{0_{2\times1}} & \mathbf{0_{2\times1}} \\ \delta_{1i} & \delta_{2i} & \delta_{3i} & 0 \end{bmatrix},$$

$$\mathbf{J}_{\mathbf{X}S4i} = 0.5\left(\mathbf{J}_{\mathbf{X}5i} + \mathbf{J}_{\mathbf{X}9i}\right) + \begin{bmatrix} \mathbf{0_{3\times6}} \\ \mathbf{J}_{\mathbf{X}\Omega1i} \end{bmatrix},$$

$$\mathbf{J}_{\mathbf{X}\Omega1i} = \begin{bmatrix} 0 & -\sin q_i \\ 0 & \cos q_i \\ 0 & 0 \end{bmatrix} \mathbf{J}_{\mathbf{X}\zeta i\varepsilon i},$$

$$\mathbf{J}_{\mathbf{Q}S3i} = 0.5\left(\mathbf{J}_{\mathbf{Q}4i} + \mathbf{J}_{\mathbf{Q}7i}\right) + \begin{bmatrix} \mathbf{0_{3\times4}} \\ \mathbf{J}_{\mathbf{Q}\Omega2i} \end{bmatrix},$$

$$\mathbf{J}_{\mathbf{Q}\Omega2i} = \begin{bmatrix} \mathbf{0_{2\times1}} & \mathbf{0_{2\times1}} & \mathbf{0_{2\times1}} & \mathbf{0_{2\times1}} \\ \delta_{1i} & \delta_{2i} & \delta_{3i} & 0 \end{bmatrix},$$

$$\mathbf{J}_{\mathbf{X}S3i} = 0.5\left(\mathbf{J}_{\mathbf{X}4i} + \mathbf{J}_{\mathbf{X}7i}\right) + \begin{bmatrix} \mathbf{0_{3\times6}} \\ J_{X\Omega2i} \end{bmatrix},$$

$$\mathbf{J}_{\mathbf{X}\Omega 2i} = \begin{bmatrix} -\sin q_i & 0 \\ \cos q_i & 0 \\ 0 & 0 \end{bmatrix} \mathbf{J}_{\mathbf{X}\zeta i\varepsilon i},$$

$$\mathbf{J}_{\mathbf{Q}S8i} = 0.5\left(\mathbf{J}_{\mathbf{Q}8i} + \mathbf{J}_{\mathbf{Q}9i}\right) + \begin{bmatrix} \mathbf{0_{3\times 4}} \\ \mathbf{J}_{\mathbf{Q}\Omega 2i} \end{bmatrix},$$

$$\mathbf{J}_{\mathbf{X}S8i} = 0.5\left(\mathbf{J}_{\mathbf{X}8i} + \mathbf{J}_{\mathbf{X}9i}\right) + \begin{bmatrix} \mathbf{0_{3\times 6}} \\ \mathbf{J}_{\mathbf{X}\Omega 2i} \end{bmatrix},$$

$$\mathbf{J}_{\mathbf{Q}S7i} = 0.5\left(\mathbf{J}_{\mathbf{Q}8i} + \mathbf{J}_{\mathbf{Q}7i}\right) + \begin{bmatrix} \mathbf{0_{3\times 4}} \\ \mathbf{J}_{\mathbf{Q}\Omega 1i} \end{bmatrix},$$

$$\mathbf{J}_{\mathbf{X}S7i} = 0.5\left(\mathbf{J}_{\mathbf{X}8i} + \mathbf{J}_{\mathbf{X}7i}\right) + \begin{bmatrix} \mathbf{0_{3\times 6}} \\ \mathbf{J}_{\mathbf{X}\Omega 1i} \end{bmatrix},$$

$$\mathbf{J}_{\mathbf{Q}S10i} = \begin{bmatrix} \frac{\partial [x_{S10i}, y_{S10i}, z_{S10i}]^{\mathrm{T}}}{\partial \mathbf{q}} \\ \mathbf{J}_{\mathbf{Q}\Omega 1i} \end{bmatrix},$$

$$\mathbf{J}_{\mathbf{Q}S2i} = \begin{bmatrix} \begin{bmatrix} 1 & 0 & 0 & 0 \\ 0 & 1 & 0 & 0 \\ 0 & 0 & 1 & 0 \end{bmatrix} \mathbf{J}_{\mathbf{Q}3i} \\ \mathbf{J}_{\mathbf{Q}\Omega 1i} \end{bmatrix},$$

$$\mathbf{F}_{\mathbf{P}} = \begin{bmatrix} m_{pl}\ddot{x} & m_{pl}\ddot{y} & m_{pl}\ddot{z} & 0 & 0 & I_{pl}\ddot{\phi} \end{bmatrix}^{\mathrm{T}},$$

$$\mathbf{F}_{ji} = m_j \begin{bmatrix} \ddot{x}_{ji} & \ddot{y}_{ji} & \ddot{z}_{ji} & 0 & 0 & 0 \end{bmatrix}^{\mathrm{T}},$$

$$\text{for } j = 2, 3, 4, 5, 7, 8, 9$$

$$\mathbf{F}_{B1i} = \begin{bmatrix} 0 & 0 & m_{B1}\ddot{q}_v & 0 & 0 & 0 \end{bmatrix}^{\mathrm{T}},$$

$$\mathbf{F}_{Bji} = \begin{bmatrix} m_{Bj}\ddot{x}_{Sji} & m_{Bj}\ddot{y}_{Sji} & m_{B2}\ddot{z}_{Sji} & 0 & 0 & I_{Bj}\ddot{q}_i \end{bmatrix}^{\mathrm{T}},$$

$$\text{for } j = 2, 10$$

$$\mathbf{F}_{Bji} = \begin{bmatrix} m_{Bj}\ddot{x}_{Sji} & m_{Bj}\ddot{y}_{Sji} & m_{B2}\ddot{z}_{Sji} & C_{Sji}^{\mathrm{T}} \end{bmatrix}^{\mathrm{T}},$$

$$\text{for } j = 3, 4, 7, 8$$

$$\begin{aligned} \mathbf{C}_{Sji} = & \left(\mathbf{R}_{\mathbf{P}qi}\mathbf{Rot}(\alpha_i, \mathbf{y}) + \mathbf{Rot}(q_i, \mathbf{z})\mathbf{R}_{\mathbf{P}\alpha i}\right) \\ & \times \mathbf{I}_{Bj}\left(\mathbf{Rot}(q_i, \mathbf{z})\mathbf{Rot}(\alpha_i, \mathbf{y})\right)^{\mathrm{T}} \Omega_{Bji} \\ & + \mathbf{Rot}(q_i, \mathbf{z})\mathbf{Rot}(\alpha_i, \mathbf{y})\mathbf{I}_{Bj}(\mathbf{R}_{\mathbf{P}qi}\mathbf{Rot}(\alpha_i, \mathbf{y}) \\ & + \mathbf{Rot}(q_i, \mathbf{z})\mathbf{R}_{\mathbf{P}\alpha i})^{\mathrm{T}}\Omega_{Bji} + \mathbf{Rot}(q_i, \mathbf{z})\mathbf{Rot}(\alpha_i, \mathbf{y}) \\ & \times \mathbf{I}_{Bj}\left(\mathbf{Rot}(q_i, \mathbf{z})\mathbf{Rot}(\alpha_i, \mathbf{y})\right)^{\mathrm{T}} \dot{\Omega}_{Bji} \end{aligned}$$

with $\alpha_i = \zeta_i$ if $j = 4, 7$, $\alpha_i = \varepsilon_i$ if $j = 3, 8$ and $\Omega_{Bji} = \begin{bmatrix} -\dot{\alpha}_i \sin q_i & \dot{\alpha}_i \cos q_i & \dot{q}_i \end{bmatrix}^{\mathrm{T}}$.

In these expressions, δ_{ij} represents the Krönecker symbol ($\delta_{ij} = 1$ if $j = i$ and $\delta_{ij} = 0$ if $j \neq i$).

References

Alba-Gomez, O., Wenger, P. and Pamanes, A. (2005). Consistent kinetostatic indices for planar 3-DOF parallel manipulators, application to the optimal kinematic inversion. *Proceedings of the ASME 2005 IDETC/CIE Conference*, Long Beach, CA, 24–28 September.

Alvan, K. and Slousch, A. (2003). On the control of the spatial parallel manipulators with several degrees of freedom. *Mechanism and Machine Theory*, **1**: 63–69.

Arakelian, V., Briot, S., Guegan, S. and Le Flecher, J. (2005). Design and prototyping of new 4-, 5- and 6-DOF parallel manipulators based on the copying properties of the pantograph linkage. *Proceedings of the 36th International Symposium on Robotics*, Tokyo, Japan, 29 November–1 December.

Arakelian, V., Briot, S. and Glazunov, V. (2006a). Singular positions of a PAMINSA parallel manipulator. *Journal of Machinery Manufacture and Reliability*, **1**: 62–69.

Arakelian, V., Maurine, P., Briot, S. and Pion, E. (2006b). Parallel robot comprising means for setting in motion a mobile element split in two separate subassemblies. Patent number FR2873317 (A1), WO 2006/021629, 27 January. http://www.wipo.int/pctdb/en/wo.jsp?WO=2006021629&IA=WO2006021629.

Arakelian, V., Briot, S. and Glazunov, V. (2008). Increase of singularity-free zones in the workspace of parallel manipulators using mechanisms of variable structure. *Mechanism and Machine Theory*, **43**(9): 1129–1140.

Bhattacharya, S., Hatwal, H. and Ghosh, A. (1998). Comparison of an exact and approximate method of singularity avoidance in platform type parallel manipulators. *Mechanism and Machine Theory*, **33**(7): 965–974.

Bonev, I. A., Zlatanov, D. and Gosselin, C. M. (2003). Singularity analysis of 3-DOF planar parallel mechanisms via Screw Theory. *Transactions of the ASME. Journal of Mechanical Design*, **125**: 573–581.

Briot, S. and Arakelian, V. (2007). Singularity analysis of PAMINSA manipulators. *Proceedings of the 12th World*

Congress in Mechanism and Machine Science, Besançon, France, 17–21 June.

Briot, S., Bonev, I. A., Chablat, D., Wenger, P. and Arakelian, V. (2007a). Self motions of general 3-RPR planar parallel robots. *The International Journal of Robotics Research*, in press.

Briot, S., Guegan, S., Courteille, E. and Arakelian, V. (2007b). On the design of PAMINSA: a new class of parallel manipulators with high-load carrying capacity. *Proceedings of the ASME 2007 IDETC/CIE Conference*, Las Vegas, NV, 4–7 September.

Collins, C. L. and Long, G. L. (1975). The singularity analysis of a parallel hand controller for force-reflected teleoperation. *IEEE Transactions on Robotics and Automation*, **11**(5): 661–669.

Dasgupta, B. and Mruthyunjaya, T. (1998a). Force redundancy in parallel manipulators: theoretical and practical issues. *Mechanism and Machine Theory*, **33**(6): 727–742.

Dasgupta, B. and Mruthyunjaya, T. (1998b). Singularity-free path planning for the Steward platform manipulator. *Mechanism and Machine Theory*, **33**(6): 711–725.

Gosselin, C. M., and Angeles, J. (1990). Singularity analysis of closed-loop kinematic chains. *IEEE Transactions on Robotics and Automation*, **6**(3): 281–290.

Glazunov, V., Kraynev, A., Bykov, R., Rashoyan, G. and Novikova, N. (2004). Parallel manipulator control while intersecting singular zones. *Proceedings of the 15th Symposium on Theory and Practice of Robots and Manipulators (RoManSy)*, CISM-IFToMM, Montreal.

Hesselbach, J., Wrege, J., Raatz A. and Becker, O. (2004). Aspects on the design of high precision parallel robots. *Assembly Automation*, **24**(1): 49–57.

Hunt, K. H. (1987). Special configurations of robot-arms via screw theory. *Robotica*, **5**: 17–22.

Kemal Ider, S. (2005). Inverse dynamics of parallel manipulators in the presence of drive singularities. *Mechanism and Machine Theory*, **40**: 33–44.

Kevin Jui, C. K. and Sun, Q. (2005). Path tracking of parallel manipulators in the presence of force singularity. *Transactions of the ASME. Journal of Dynamic Systems, Measurement and Control*, **127**: 550–563.

Khalil, W. and Guégan, S. (2002). A novel solution for the dynamic modeling of Gough-Stewart manipulators. *Proceedings of the IEEE International Conference on Robotics and Automation*, Washington, DC, 11–15 May.

Kim, H. S. and Choi, Y. J. (2001). Forward/inverse force transmission capability analyses of fully parallel manipulators. *IEEE Transactions on Robotics and Automation*, **17**(4): 526–531.

Kim, S.-G. and Ryu, J. (2004). Force transmission analyses with dimensionally homogeneous Jacobian matrices for parallel manipulators. *KSME International Journal*, **18**(5): 780–788.

Lee, S.-H., Song, J.-B., Choi, W. C. and Hong, D. (2002). Workspace and force-moment transmission of a variable arm type parallel manipulator. *Proceedings of the IEEE International Conference on Robotics and Automation*, Vol. 4, pp. 3666–3671.

Liu, X.-J., Wang, J. and Pritschow, G. (2006). Kinematics, singularity and workspace of planar 5R symmetrical parallel mechanism. *Mechanism and Machine Theory*, **41**(2): 119–144.

Ma, O. and Angeles, J. (1992). Architecture singularities of parallel manipulators. *The International Journal of Robotics and Automation*, **7**(1): 23–29.

Merlet, J.-P. (1989). Singular configurations of parallel manipulators and Grassmann geometry. *The International Journal of Robotics Research*, **8**(5): 45–56.

Merlet, J.-P. (2006). *Parallel Robots*, 2nd edition. Berlin, Springer.

Nenchev, D. N., Bhattacharya, S. and Uchiyama, M. (1997). Dynamic analysis of parallel manipulators under the singularity-consistent parameterization. *Robotica*, **15**(4): 375–384.

Ottaviano, E., Gosselin, C. M. and Ceccarelli, M. (2001). Singularity analysis of CaPaMan: a three-degree of freedom spatial parallel manipulator. *Proceedings of the 2001 IEEE International Conference on Robotics and Automation*, Seoul, Korea, 21–26 May, pp. 1295–1300.

Perng, M. H., and Hsiao, L. (1999). Inverse kinematic solutions for a fully parallel robot with singularity robustness. *The International Journal of Robotics Research*, **18**(6): 575–583.

Seyferth, W. (1974). Massenersatz duch punktmassen in räumlichen getrieben. *Mechanism and Machine Theory*, **9**: 49–59.

Weiwei, S. and Shuang, C. (2006). Study on force transmission performance for planar parallel manipulator. *Proceedings of the World Congress on Intelligent Control and Automation (WCICA)*, Vol. 2, pp. 8098–8102.

Wen, J. T. and Oapos Brien, J. F. (2003). Singularities in three-legged platform-type parallel mechanisms. *IEEE Transactions on Robotics and Automation*, **19**(4): 720–726.

Wu, Y., and Gosselin, C. M. (2007). On the dynamic balancing of multi-DOF parallel mechanisms with multiple legs. *Transactions of the ASME. Journal of Mechanical Design*, **129**(2): 234–238.